

## Microstructural evolution of gas atomized Al–Zn–Mg–Cu–Zr powders during semi-solid rolling process

Feng-xian LI<sup>1,2</sup>, Yun-zhong LIU<sup>2</sup>, Jian-hong YI<sup>1</sup>

1. College of Materials Science and Engineering, Kunming University of Science and Technology, Kunming 650033, China;
2. College of Mechanical and Automotive Engineering, South China University of Technology, Guangzhou 510640, China

Received 24 July 2013; accepted 12 December 2013

**Abstract:** Under H<sub>2</sub> atmosphere, the green strips were prepared from Al–5.8Zn–1.63Mg–2.22Cu–0.12Zr (mass fraction, %) powders by the semi-solid rolling process with a relative density from 76.1% to 88.0%. The role of temperature on microstructure and mechanical properties was investigated. With increasing rolling temperature from 580 to 610 °C, the disappearance of primary powder boundary and isolated pores, inter-diffusion of species and the change of grain boundary were accelerated. Moreover, the mechanism of microstructure evolution changes from the densification dominant regime to the coarsening dominant regime; the amount of  $\eta$  (MgZn<sub>2</sub>) phase decreased and more Al<sub>2</sub>Cu particles precipitated at grain boundaries. The optimum temperature for semi-solid rolling of Al–5.8Zn–1.63Mg–2.22Cu–0.12Zr powders was determined. The liquid fraction in the range of 53% to 67% corresponds with a high density level of green strips. The present experimental analysis suggests that semi-solid powder rolling can be optimized to manufacture strips with high mechanical properties.

**Key words:** semi-solid rolling; aluminum alloy powder; microstructure

### 1 Introduction

The process of metal powder rolling in the semi-solid temperature range is attractive due to its conceptual simplicity and economical operation cost. This process shows promise for providing a new method of strip production with energy and materials saving, short production run for the metal processing industry.

Inspecting the available literature, the aluminum alloy strips can be prepared by different methods. HAGA and SUZUKI [1] devised a melt drag twin roll caster in order to cast aluminum alloy strips at a higher speed. This method could cast thinner strips than the conventional twin roll caster for aluminum alloys. Thixo-rolling is widely used to produce strips [2,3]. In 2003, spray rolling proposed by MCHUGH et al [4] provided a new method of strip production for the metal industry. However, little information has been obtained for this new strip manufacturing process, which limits its industrial application. Usually, materials in the form of

powders are compacted through powder metallurgy, hot rolling and spark plasma extrusion to acquire fine microstructures with unique properties [5–8].

However, it should be noted that the previous work only focused on a lower forming temperature compared with semi-solid rolling. An understanding of the microstructural evolution of gas atomized metal powders during semi-solid rolling is still lacking. The semi-solid rolling process involves high-temperature applications affecting the microstructure of the bulks, thus altering the mechanical properties. Therefore, it is necessary to analyze the relationships between the forming temperature and microstructures, and facilitate a full control over the processes in terms of properties.

The aim of this research is to investigate microstructural evolution of gas atomized Al–5.8Zn–1.63Mg–2.22Cu–0.12Zr (mass fraction, %) powders during semi-solid rolling. Moreover, this work emphasizes the influence of liquid fraction formed in the remelting process on the microstructures and mechanical properties of green strips.

## 2 Experimental

In this work, semi-solid rolling experiments were carried out on atomized powders with composition of Al–5.8Zn–1.63Mg–2.22Cu–0.12Zr (mass fraction, %).

All the powder particles were spherical in shape (Fig. 1(a)). The size distribution of the atomized powders was carried out by laser diffraction technique using the Mastersizer 2000 particle size analyzer. Figure 1(b) illustrates the log normal and cumulative size distribution of the gas atomized powders. A broad size distribution of the powders can improve the packing density. The mass median diameter of the particles is 65  $\mu\text{m}$ . The cumulative size distribution indicates  $D_{10}$ =14.2  $\mu\text{m}$ ,  $D_{50}$ =41.2  $\mu\text{m}$  and  $D_{90}$ =87.5  $\mu\text{m}$  corresponding to the particle sizes at 10%, 50% and 90%, respectively. Differential thermal analysis (DTA) was performed with a Netzsch STA 449C at a scan rate of 10  $^{\circ}\text{C}/\text{min}$ . The rolls used are of 150 mm in diameter and 100 mm in length. The rolls were rotated at 31.8 mm/s, and preheated to a temperature about 230  $^{\circ}\text{C}$ . In order to understand the effect of high temperature on the microstructures, metal powders were heated at 580, 600, 610 and 620  $^{\circ}\text{C}$  for 30 min in a furnace under  $\text{H}_2$  atmosphere. And metal powders were heated at 610  $^{\circ}\text{C}$

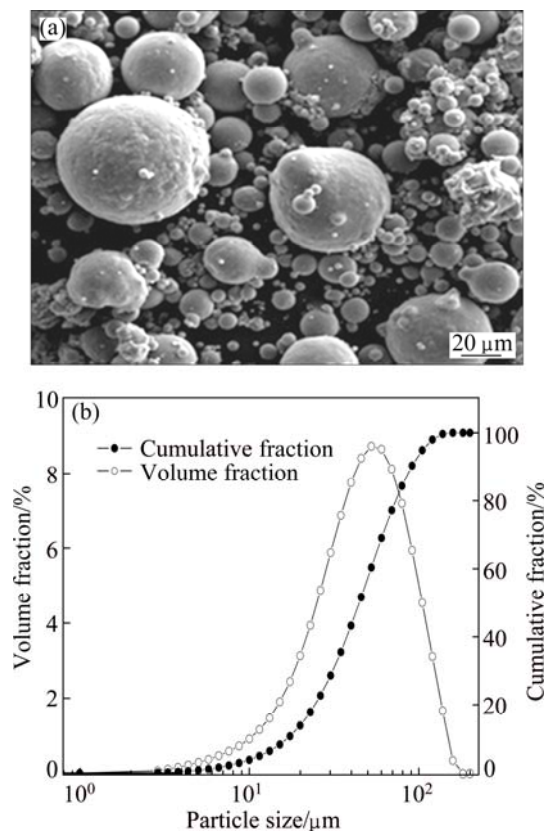


**Fig. 1** Morphology (a) and log normal and cumulative size distribution (b) of gas atomized Al–5.8Zn–1.63Mg–2.22Cu–0.12Zr powders

for 10, 20, 30 and 40 min. The powder is naturally supplied into the roll gap by gravity. Then strips were produced up to 100 mm in width and 0.7 mm in thickness. The solution treatment is usually carried out at the highest temperature possibly without remelting. The following recipes were used: solution treatment (471  $^{\circ}\text{C}$ , 2 h)→aging (125  $^{\circ}\text{C}$ , 12 h+166  $^{\circ}\text{C}$ , 15 h).

Longitudinal cross-sections of the green strips under different temperatures were polished. Keller's etchant was used to reveal grain structure and highlight constituent phases. Crystal structure was characterized by X-ray diffractometer (XRD) using high energy monochromatic radiation in the  $2\theta$  range from 10  $^{\circ}$  to 90 $^{\circ}$  at a scan rate of 17.7 s/step, the morphology and cross-sectional microstructure of the green strips were observed by the Nova Nano SEM430 scanning electron microscope (SEM). Relative density can be measured with a buoyancy weighting machine. The theoretical density of Al–5.8Zn–1.63Mg–2.22Cu–0.12Zr alloy is 2.281  $\text{g}/\text{cm}^3$ . Vickers hardness of the specimen was measured by the HVs-100 Vickers hardness tester applying the load of 0.98 N for 15 s. The values were averaged.

## 3 Results and discussion

### 3.1 Microstructural evolution under different forming temperatures

DTA analysis was performed on samples of gas atomized Al–5.8Zn–1.63Mg–2.22Cu–0.12Zr powders. Scan data and peak assignments for gas atomized powders are summarized in Fig. 2(a). The solidus–liquidus temperature of gas atomized Al–5.8Zn–1.63Mg–2.22Cu–0.12Zr powders ranges from 520 to 640  $^{\circ}\text{C}$ . Because the rolling temperature is above the solid temperature of the powders, different volume fractions of liquid would exist in the powder. The relationship between temperature and solid fraction is shown in Fig. 2(b). It can be seen that the solid fraction decreases from 86% to 35% with increasing temperature from 580 to 620  $^{\circ}\text{C}$ .

Figure 3 presents the microstructures of green strips after semi-solid rolling at different temperatures from Al–5.8Zn–1.63Mg–2.22Cu–0.12Zr powders. At semi-solid temperature of 580  $^{\circ}\text{C}$ , namely solid fraction  $f_s$  is 86% (Fig. 3(a)), the powders maintain their shapes, and the primary particle boundaries can be seen.

The microstructure was also characterized by grain structure with random, isolated pores of various shapes.

An increase in rolling temperature (600  $^{\circ}\text{C}$ , namely solid fraction  $f_s$  is 67%) points to the development of metal contact between particles (Fig. 3(b)). The primary powder boundaries in the plane of contact are disintegrated, which leads to a decrease in surface to

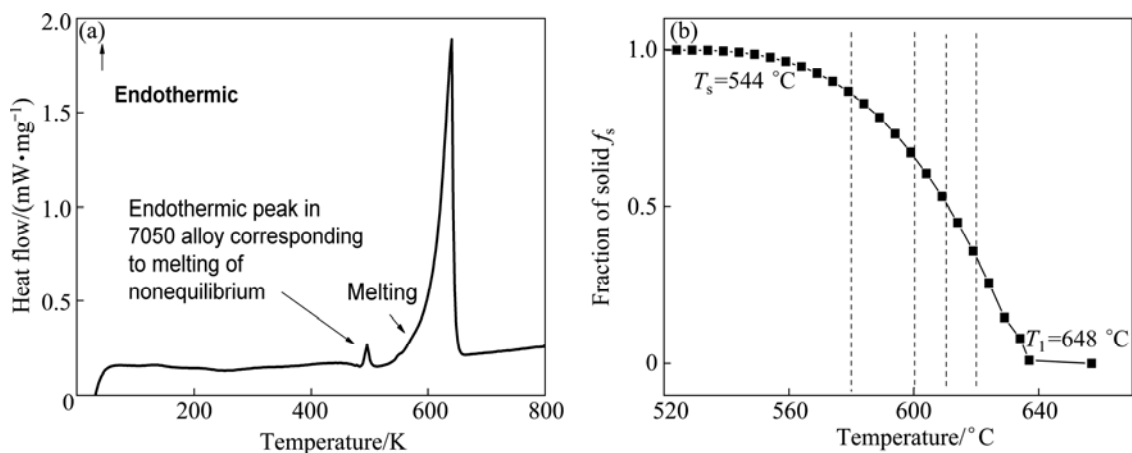


Fig. 2 Differential thermal analysis (a) and solid fraction against temperature (b) of Al-5.8Zn-1.63Mg-2.22Cu-0.12Zr powders

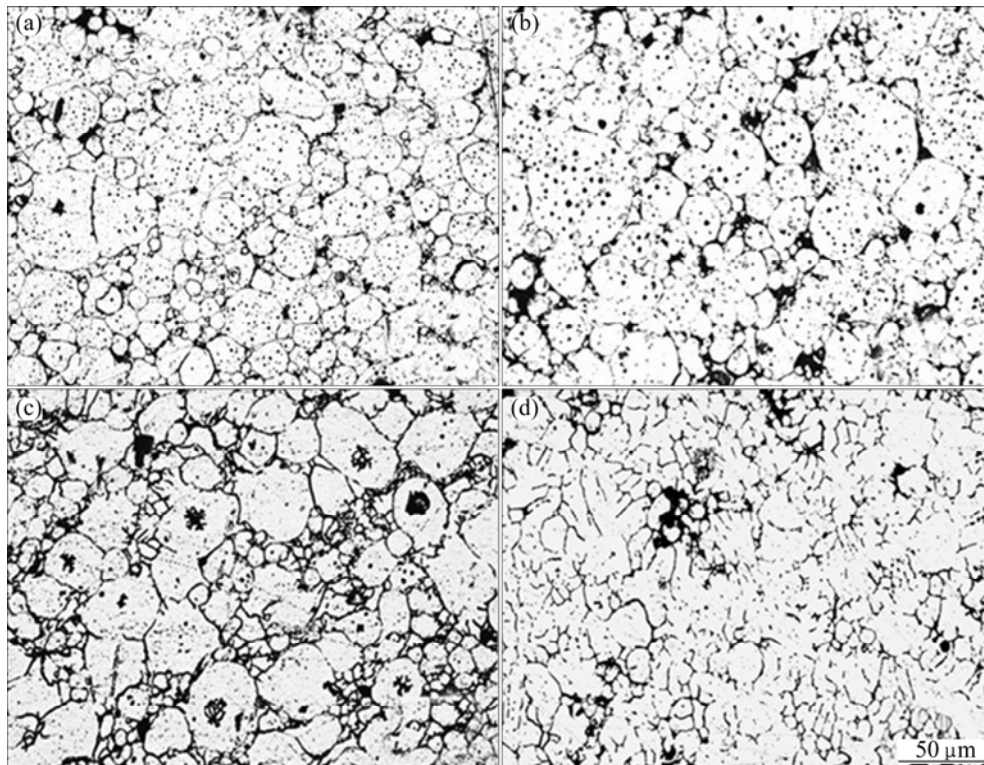


Fig. 3 Microstructures of green strip semi-solid rolled at different temperatures: (a) 580 °C; (b) 600 °C; (c) 610 °C; (d) 620 °C

volume ratio and thus a decrease in free energy of the system. It is evident that powders are joined to a distance at which physical interaction arises or weak chemical interaction arises. Moreover, some liquid pockets are present within the primary phase. With a high solid fraction ( $f_s > 67\%$ ), it can be seen that semi-solid powder rolling shares many similarities compared with hot rolling [9,10]. At 610 °C, a few powder primary boundaries change greatly (Fig. 3(c)). This can be attributed to the liquid in the process of penetrating, namely, the solid fraction can reach approximately 53%. At the heating temperature of 620 °C (Fig. 3(d)), the strip is characterized by a dendritic type structure.

As illustrated above, it can be concluded that high temperature can accelerate the disappearance of primary particle boundary in the plane of contact and the change of powder primary boundaries, which give evidence of an interlocking between particles under high-temperature condition. There are some factors that can illustrate the feasibility of semisolid processing for obtaining the advantages of powder rolling and semi-solid rolling: 1) At temperatures like 600 and 610 °C, the material seems to have been effectively processed in a semisolid state, namely judging by the appearance of the microstructures (Fig. 3), the materials are partial melting; 2) The directive evidence of the liquid penetrating the particles

boundaries is observed; 3) Moreover, the microstructure of the semi-solid sample is non-dendritic at appropriate solid fraction.

### 3.2 Grain boundary diffusion in primary phase

Note examples of liquid in the process of penetrating down grain boundaries, as shown in Fig. 3(c), the following tests were carried out to investigate the effect of heating the powder at 610 °C ( $f_s$  is 53%) for different holding time on the microstructure evolution of strips.

In Fig. 4 (a), a large liquid part is apparent to detach itself from the particles' boundary (indicated by arrow *A*), and another one is going to form from the liquid in the grain (indicated by arrow *B*). This kind of powders with short holding time has undergone a lesser degree of particle boundary change than the powder with long holding time as shown in Fig. 4(b). This phenomenon, liquid penetrating down boundaries, is similar to the primary rearrangement during liquid phase sintering, i.e. the liquid penetrating into the solid particles [11].

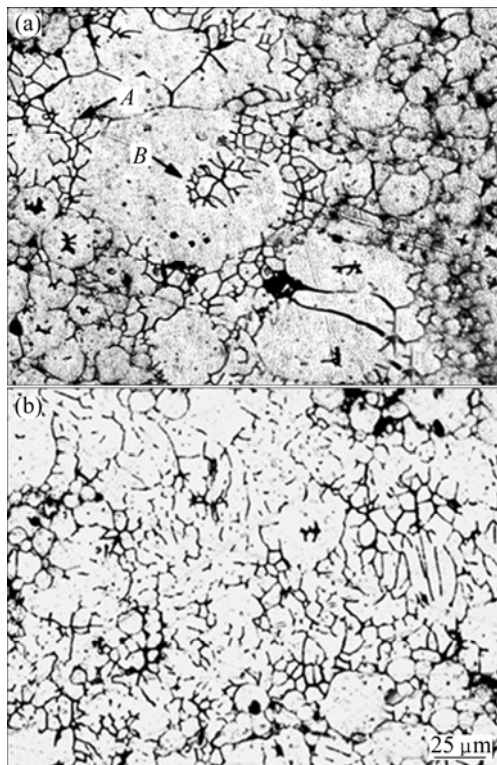


Fig. 4 Microstructures of strip semi-solid rolled at 610 °C for different holding time: (a) 10 min; (b) 30 min

The degree of liquid penetration depends on the local balancing of surface energies [12]. In gas atomized powders, the solidification of liquid metal droplets has a significant effect on the microstructure. The powders are in a non-equilibrium state due to rapid solidification process. Moreover, grain rotation is prohibitive by the high-volume fraction of solid, and grain orientation is

random. As the temperature is increased, there has been a tendency in establishing equilibrium after the initial liquid formation, and mass in each of the two adjacent particles transports from the grain boundary to the contact surface via diffusion. Once the energy between the adjoining particles exceeds an energy barrier for the movement of the grain boundary, the grain boundaries change greatly.

As illustrated above, it can be also seen that pore shrinkage and disappearance may occur simultaneously as processing temperature and holding time are increased. Pores were formed in gas atomized powders by dissolution of gas from the molten metal, gas entrapment during droplet forming and solidification shrinkage. As temperature increases, pores disappear by moving through the liquid phase in the semi-solid material. LANGE et al [13] pointed out that the pore closure is controlled by the number of grain boundaries. It was postulated that the greater the number of grain boundaries intercepting the pore is, the greater the number of rapid paths for mass transport is, the faster the mass can be derived to the pore, thus the greater the rate of pore disappearance is.

### 3.3 Mechanical properties of strips

Figure 5 shows the relative density and Vickers hardness of the green strip after semi-solid rolling at different temperatures. The density of the rolled material increases with increasing temperature. The relative density of 88.0% was obtained in the strip semi-solid rolled at 610 °C, while in the case of 580 °C it was 76.1 %. BHUIYAN et al [14] also observed the same phenomenon in the heat-treated gas atomized *n*-type 95%Bi<sub>2</sub>Te<sub>3</sub>–5%Bi<sub>2</sub>Se<sub>3</sub> thermoelectric powders. Density changes are taking place as a function of the amount of material melted.

The Vickers hardness of Al–5.8Zn–1.63Mg–2.22Cu–0.12Zr powders is about HV 168.9. And the

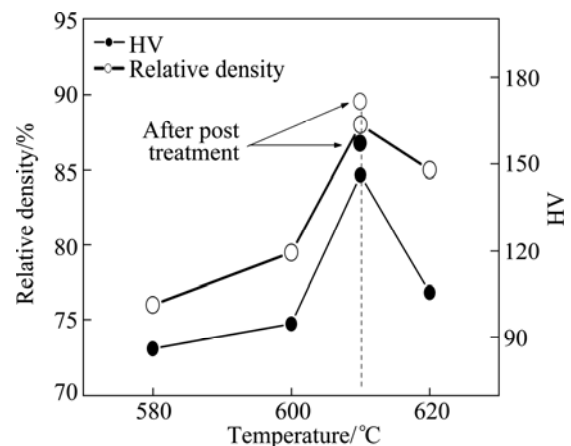


Fig. 5 Relative density and Vickers hardness of green strip under different temperatures

Vickers hardness of full density bulk materials is HV 188.5. It is interesting to note that the Vickers hardness increases fast with increasing rolling temperature, arriving at HV 146.3 at 610 °C, which is almost double compared with that at 580 °C at the given roll setting. It can be seen that the Vickers hardness is increased due to the dense structure. Moreover, being of the Al–Zn–Mg–Cu series, this aluminum alloy is heat treatable, hence besides melting, an influence of precipitated phases on the Vickers hardness should be also considered.

The SEM images of the specimens rolled at different forming temperatures are summarized in Fig. 6. The microstructure presented in Fig. 6 (a) clearly shows that some liquid pockets and porosity retain when the strip is semi-solid rolled at 580 °C. In Fig. 6(b), the particles which distribute along the grain boundary are ascertained as  $\eta$  ( $\text{MgZn}_2$ ) and  $\text{AlCu}_2$ , according to XRD (see Fig. 7) and energy dispersive spectroscopy (EDS) results (see Table 1), as well as the report in Ref. [15]. Al–5.8Zn–1.63Mg–2.22Cu–0.12Zr powders, along with many Al–Zn–Mg–Cu alloys with more than 1% copper, also precipitate  $\text{CuMgAl}_2$  phase [15]. However, the diffraction peak assigned to  $\text{CuMgAl}_2$  phase cannot be detected due to the limit amount. As shown in Fig. 6(c), many grain boundaries change due to high temperature. Obviously, the diffraction peak assigned to  $\eta$  ( $\text{MgZn}_2$ ) phases can only be detected from the 580 °C, 30 min and 600 °C, 30 min treated particles. Moreover, the diffraction intensity of  $\eta$ ( $\text{MgZn}_2$ ) phase decreases owing

to dissolution into  $\alpha$ (Al) solid solution. In the semi-solid rolled strip at 620 °C, the bright particles identified as  $\text{Al}_2\text{Cu}$  precipitated at grain boundaries. This behavior also indicates the participation of Cu from the Al matrix as the temperature increases. Figure 6(d) shows a homogeneous distribution of particles in the structure of green strips after post treatment compared with the structure of green strips. These particles are formed by decomposition of a super saturated solid solution during age hardening. The fine precipitates are responsible for the high strength of alloys. The Vickers hardness and relative density increase to HV 158.3 and 91.6%, respectively, as shown in Fig. 5.

It can be concluded that the changes in volume fraction, distribution, and morphology of the strengthening phase with the rolling temperature have remarkable influence on the mechanical properties of strips.

Referring to Table 1, and as expected from the processing conditions, metal powders were heated under  $\text{H}_2$  atmosphere, an increased amount of oxidation is still observed as processing temperature is raised. The oxygen exists at the grain boundary after semi-solid rolling at 580 °C and 600 °C, respectively. When the temperature reaches 610 °C, more oxygen can be detected at the grain boundary. The oxygen at the grain boundary may participate from the Al matrix as the temperature increases or may come from the powders or surface oxide film, i.e. powders adsorbed oxygen. These oxides must certainly act as diffusion barriers for the

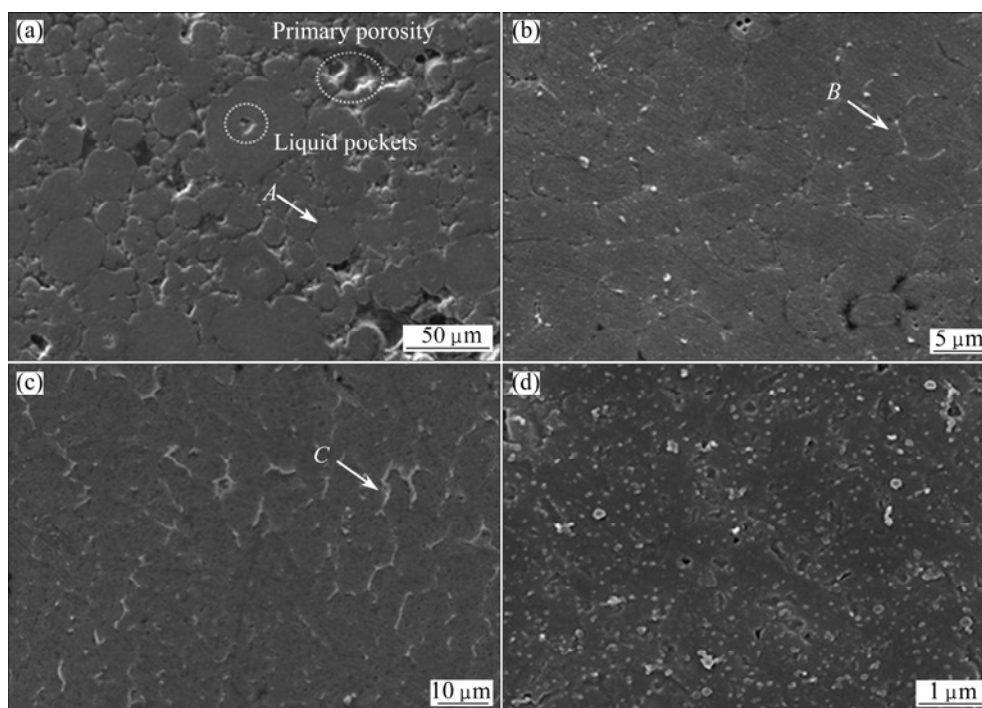


**Fig. 6** SEM images of green strip rolled at different temperatures: (a) 580 °C, 30 min; (b) 600 °C, 30 min; (c) 620 °C, 30 min; (d) 610 °C, 30 min and post-treatment

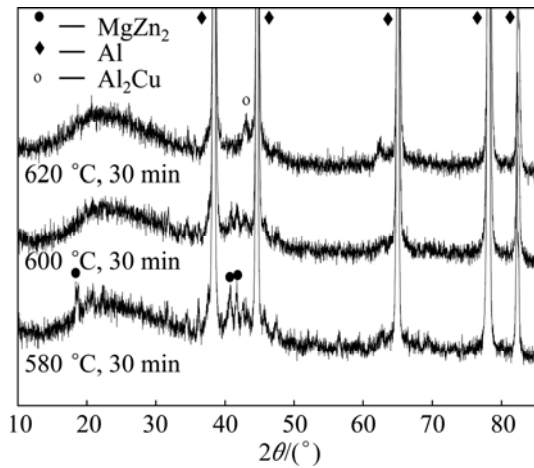


Fig. 7 XRD patterns of compact

Table 1 EDS analysis results of green strips semi-solid rolled at different temperatures from gas atomized powders

Area in Fig. 6	w(O)/%	w(Mg)/%	w(Al)/%	w(Cu)/%	w(Zn)/%
A	1.75	1.96	87.99	2.32	5.98
B	1.83	1.83	89.78	3.42	4.14
C	1.92	–	67.52	31.56	–

formation of sintering necks between particles. And the oxygen content of powder is responsible for the formation of grain boundary networks [16]. However, the disappearance of primary particle boundary in the plane of contact and the change of powder primary boundaries when the material is partially melted evident that the effect of oxygen content on impeding or preventing the diffusion between the primary

particles is limited.

### 3.4 Development trend of microstructure

The microstructural evolution of green strip during semi-solid rolling from gas atomized powders can be divided into two stages with respect to temperature (Fig. 8), which respectively correspond to either a densification dominant regime or coarsening dominant regime. Note that  $f_s$  greater than 61% corresponds to densification dominant regime, i.e. the presence of porosity and the disappearance of primary particle boundary in the plane of contact. Nevertheless,  $f_s$  less than 61% corresponds to coarsening dominant regime, i.e. primary particles boundary networks diffused, and the grain boundary changed. Because the quantity of liquid is high, the effect of the presence of prior particles boundary networks and particles on the migration of liquid film grain boundaries is limited. Therefore, grain growth and grain coarsening are caused enviably [17,18]. Moreover, there will be problems of process control. When the material has been melted fully, it finally presents an as-cast microstructure.

Because of the presence of a uniform distribution of liquid, density and hardness, the optimum semi-solid forming temperature for Al–5.8Zn–1.63Mg–2.22Cu–0.12Zr powder is suggested between 600 °C and 610 °C, namely, the amount of solid formed in powder material is between 53% and 67%. Holding time for Al–Zn–Mg–Cu alloys should be minimal enough to ensure thermal equilibrium and the presence of a uniform distribution of liquid. It is suggested between 20 min and 30 min. While still in the early stages of development, semi-solid powder rolling shows feasibility for producing strip.

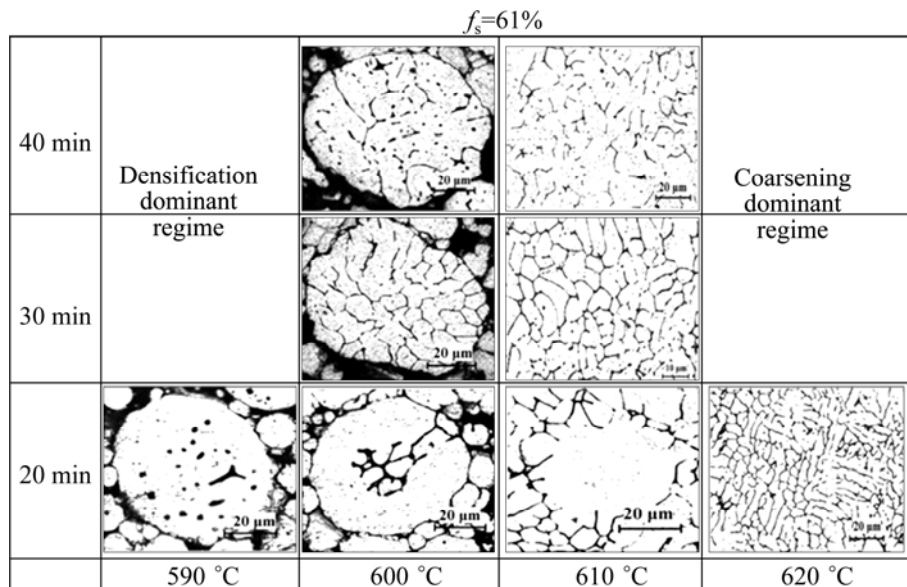


Fig. 8 Illustration of representative microstructure

## 4 Conclusions

1) The temperature has a significant effect on the disappearance of prior boundary and inter-diffusion of species, the change of grain boundaries and the disappearance of isolated pores, which depends on the final densification and the final mechanical properties.

2) With a decrease in solid fraction, the microstructure evolution mechanism changes from the densification dominant regime to the coarsening dominant regime, and the density of the green strip grows and the micro hardness of strips is improved. Moreover, the amount of  $\eta$  ( $\text{MgZn}_2$ ) phase decreases, and more particles  $\text{Al}_2\text{Cu}$  precipitate at the grain boundaries.

3) The optimum semi-solid forming temperature for  $\text{Al-5.8Zn-1.63Mg-2.22Cu-0.12Zr}$  powders is suggested between  $600\text{ }^\circ\text{C}$  and  $610\text{ }^\circ\text{C}$ , namely the liquid fraction in the range of 53% to 67% corresponds with a high density level of green strips.

## References

- [1] HAGA T, SUZUKI S. A high speed twin roll caster for aluminum alloy strip [J]. *Journal of Materials Processing Technology*, 2001, 113: 291–295.
- [2] BIROL Y. Response to T6 heat treatment of extruded and thixoformed EN AW 2014 alloys [J]. *Materials Science and Engineering A*, 2011, 528: 5636–5641.
- [3] SINGER A R E. The principle of spray rolling of metals [J]. *Metallurgical Materials*, 1970, 4: 246–250.
- [4] MCHUGH K M, LIN Y, ZHOU Y, JOHNSON S B, DELPLANQUE J P, LAVERNIA E J. Microstructure evolution during spray rolling and heat treatment of 2124 Al [J]. *Materials Science and Engineering A*, 2008, 477: 26–34.
- [5] RAHIMIANA M, PARVINB N, EHSANIA N. Investigation of particle size and amount of alumina on microstructure and mechanical properties of Al matrix composite made by powder metallurgy [J]. *Materials Science and Engineering A*, 2010, 527: 1031–1038.
- [6] MANN R, HEXEMER J R, DONALDSON I W, BISHOP D P. Hot deformation of an Al–Cu–Mg powder metallurgy alloy [J]. *Materials Science and Engineering A*, 2011, 528: 5476–5483.
- [7] ZABIHI M, TOROGHINOJAD M R, SHAFYEI A. Application of powder metallurgy and hot rolling processes for manufacturing aluminum/alumina composite strips [J]. *Materials Science and Engineering A*, 2013, 560: 567–574.
- [8] MORSIA K, ESAWIB A, BORAHA P, LANKAA S, SAYEDB A, TAHERB M. Properties of single and dual matrix aluminum–carbon nanotube composites processed via spark plasma extrusion (SPE) [J]. *Materials Science and Engineering A*, 2010, 527: 5686–5690.
- [9] VAJPAI S K, DUBE R K, SANGAL S. Microstructure and properties of Cu–Al–Ni shape memory alloy strips prepared via hot densification rolling of argon atomized powder preforms [J]. *Materials Science and Engineering A*, 2011, 529: 378–387.
- [10] WEGMANN G, GERLING R, SCHIMANSKY F P, ZHANG J X. Spray forming and subsequent forging of  $\gamma$ -titanium aluminum alloys [J]. *Materials Science and Engineering A*, 2002, 329–331: 99–105.
- [11] YU F X, CUI J Z, RANGATHAN S, DWARAKADASA E S. Fundamental differences between spray forming and other semisolid processes [J]. *Materials Science and Engineering A*, 2001, 304–306: 621–626.
- [12] GERMAN M R. Super solidus liquid phase sintering. I: Process review [J]. *International Journal of Powder Metallurgy*, 1990, 26: 23–34.
- [13] LANGE F F. Densification of powder compacts: An unfinished story [J]. *Journal of the European Ceramic Society*, 2008, 28: 1509–1516.
- [14] BHUIYAN M H, KIM T S, KOO J M, HONG S J. Microstructural behavior of the heat treated *n*-type 95% $\text{Bi}_2\text{Te}_3$ –5% $\text{Bi}_2\text{Se}_3$  gas atomized thermoelectric powders [J]. *Journal of Alloys and Compounds*, 2011, 509: 1722–1728.
- [15] NING Z L, GUO S, CAO F Y, WANG G J, LI Z C, SUN J F. Microstructural evolution during extrusion and ECAP of a spray deposited Al–Zn–Mg–Cu–Sc–Zr alloy [J]. *Journal of Materials Science*, 2010, 45: 3023–3029.
- [16] DELPLANQUE J P, LAVERNIA E J, RANGE R H. Analysis of in-flight oxidation during reactive spray atomization and deposition processing of aluminum [J]. *Journal of Heat Transfer-TASM*, 2000, 122: 126–133.
- [17] LANGE F F. Powder processing science and technology for increase reliability [J]. *Journal of the American Ceramic Society*, 1989, 72: 3–15.
- [18] ATKINSON H V, LIU D. Microstructural coarsening of semi-solid aluminium alloys [J]. *Materials Science and Engineering A*, 2008, 496: 439–446.

# 气雾化 Al–Zn–Mg–Cu–Zr 粉 在半固态轧制过程中显微组织的演变

李凤仙<sup>1,2</sup>, 刘允中<sup>2</sup>, 易健宏<sup>1</sup>

1. 昆明理工大学 材料科学与工程学院, 昆明 650033; 2. 华南理工大学 机械与汽车工程学院, 广州 510640

**摘要:** 在  $\text{H}_2$  气氛下, 采用半固态轧制工艺将  $\text{Al-5.8Zn-1.63Mg-2.22Cu-0.12Zr}$  (质量分数) 粉末成功轧制成相对密度为 76.1%~88.0% 的生带材。分析了温度对生带材显微组织和力学性能的影响规律。当轧制温度由  $580\text{ }^\circ\text{C}$  上升到  $610\text{ }^\circ\text{C}$  时, 加速了原始颗粒边界和内部孔洞的消失、粒子的扩散、晶界的变化; 显微组织演变的机制由致密为主的阶段转变为以晶粒粗化为主的阶段;  $\eta$  ( $\text{MgZn}_2$ ) 相的数量在减少, 更多的  $\text{Al}_2\text{Cu}$  粒子在晶界处析出。获得了  $\text{Al-5.8Zn-1.63Mg-2.22Cu-0.12Zr}$  (质量分数) 粉末的最佳半固态轧制温度。当液相分数为 53%~67% 时可以制备出具有较高密度的生带材。该研究有助于采用半固态轧制将金属粉末制备出性能较好的带材。

**关键词:** 半固态轧制; 铝合金粉末; 显微组织

(Edited by Xiang-qun LI)